How to cite: *Angew. Chem. Int. Ed.* **2022,** *61,* e202206926
International Edition: doi.org/10.1002/anie.202206926
German Edition: doi.org/10.1002/ange.202206926

Cofactor Recycling | Hot Paper

A Versatile Chemoenzymatic Nanoreactor that Mimics NAD(P)H Oxidase for the In Situ Regeneration of Cofactors

*Andoni Rodriguez-Abetxuko, Antonio Reifs, Daniel Sánchez-deAlcázar, and Ana Beloqui**

Abstract: Herein, we report a multifunctional chemoenzymatic nanoreactor (NanoNOx) for the glucose-controlled regeneration of natural and artificial nicotinamide cofactors. NanoNOx are built of glucose oxidase-polymer hybrids that assemble in the presence of an organometallic catalyst: hemin. The design of the hybrid is optimized to increase the effectiveness and the directional channeling at low substrate concentration. Importantly, NanoNOx can be reutilized without affecting the catalytic properties, can show high stability in the presence of organic solvents, and can effectively oxidize assorted natural and artificial enzyme cofactors. Finally, the hybrid was successfully coupled with NADH-dependent dehydrogenases in one-pot reactions, using a strategy based on the sequential injection of a fuel, namely, glucose. Hence, this study describes the first example of a hybrid chemoenzymatic nanomaterial able to efficiently mimic NOx enzymes in cooperative one-pot cascade reactions.

Dehydrogenases (DHs) show enormous potential in the chemical, pharmaceutical, and food industry, as they catalyze redox reactions with high selectivity and efficiency under ambient conditions.[1] However, most of them require the use of small and expensive molecules as co-substrates, namely, cofactors such as nicotinamide adenine dinucleotides (NAD(P)s), to carry out the catalysis. The development of efficient cofactor recycling systems is therefore critical to assess the economic viability and the catalytic performance of DHs in high-scale oxidative biotransformations.[2,3] In this regard, Nature has designed extraordinary biomolecules, NAD(P)H oxidases (NOx), which, in combination with DHs, accomplish a cost-effective enzymatic cofactor recycling system. Nevertheless, NOx enzymes present several shortcomings such as poor operational stability, the need for other cofactors (e.g., flavin adenine dinucleotides), low activity in the presence of organic solvents, and high specificity towards non-phosphorylated natural nicotinamides. The latter frustrates the combination of NOx with NADPH-dependent enzymes in a multitude of redox applications.[4,5] As an alternative to Nature's design, a wide array of artificial systems has recently emerged, including chemo-,[6] electro-,[7] photo-,[8] and hybrid, i.e., photobiocatalytic[9] approaches. Such artificial systems are generally robust, manipulable materials that enable the transformation of either natural or artificial cofactors. Yet, in combination with DHs, the recycling performance of these materials is significantly lower than the natural NOx-DH enzyme pair.[2] Therefore, there is a demand for novel strategies to improve the performance of artificial NOx as efficient cofactor recycling systems.

The use of hemin as active catalytic core of biomimetic NOx systems has been demonstrated to be successful for the oxidation of NADH.[10–12] Hemin is an organometallic iron (III) porphyrin that requires embedment into stabilizing scaffolds due to its inherent hydrophobicity and concomitant low stability in aqueous systems.[13,14] Although hemin-based materials effectively peroxidize enzymatic cofactors, they have shown strong limitations when coupled to enzymes. To the best of our knowledge, there are no examples in which the full recycling system, i.e., DHs plus artificial hemin-based NOx mimetics, has been proven effective.[10] This drop of interest in hemin-based materials might be determined by the addition of hydrogen peroxide as a co-substrate to oxidize the cofactor. The accumulation of hydrogen peroxide in the reaction medium can poison and concomitantly inactivate both the DH enzyme and the hemin itself.[15] In this regard, experimental designs that hold the concentration of the hydrogen peroxide low, together with the development of supramolecular approaches that foster the activity of hemin molecules and protect the (bio)catalyst from inactivation, are of high interest.[16]

The arrangement of (bio)catalysts in spatially confined environments is currently being explored to facilitate the design of efficient chemical reactions.[17,18] Confined architectures seek for the optimization of the substrate-product diffusion pathways, which ameliorates the overall catalytic activity of multicatalytic systems and reduces mutual-inactivation events.[19,20] Particularly, we have focused our

[*] A. Rodriguez-Abetxuko, A. Reifs
CIC nanoGUNE, Basque Research and Technology Alliance (BRTA)
Tolosa Hiribidea 76, 20018 Donostia-San Sebastián (Spain)
Dr. D. Sánchez-deAlcázar, Dr. A. Beloqui
POLYMAT and Department of Applied Chemistry,
University of the Basque Country UPV/EHU
Paseo Manuel Lardizabal 3, 20018 Donostia-San Sebastián (Spain)
E-mail: ana.beloquie@ehu.eus
Dr. A. Beloqui
IKERBASQUE
Plaza Euskadi 5, 48009 Bilbao (Spain)

interest on the design of hybrid chemoenzymatic materials that allow the colocalization of active (bio)catalytic centers in the nanospace.[21,22] Specifically, our system localizes hemin catalysts on the surface of glucose oxidase (GOx) to give rise to manipulable and integrated nanoreactors that display Nox-like activity. Such hybrid systems, which we named NanoNOx, are formed by the assembly of GOx enzymes individually wrapped by a catalytic polymer. The shell is composed by a porous nanogel decorated with imidazole motifs that anchor and allocate hemin catalysts around the enzyme. Importantly, imidazole molecules insert in the coordination sphere of the iron porphyrin catalyst as proximal ligands, thereby boosting its catalytic performance.[23] With this confined distribution, NanoNOx are all-in-one hybrid systems in which the GOx enzyme supplies in situ the required co-substrate, i.e., H_2O_2, to the organometallic catalyst. Interestingly, the use of NanoNOx combined with a stepwise fuel injection strategy, overcomes the main issue of reported hemin-based Nox mimetics, demonstrating success as an in situ recycling system in combination with DHs (Scheme 1).

The fabrication of the nanogel has been optimized from a reported protocol in order to achieve heterogeneous catalysts.[24–26] Synthesis procedures and characterization of the material are documented in detail in the Supporting Information section (Figure S1 to S9 and Table S1). A long-term storage stability and the kinetic profile of the Nox-like activity of heterogeneous NanoNOx were experimentally revealed under aerobic conditions in the presence of glucose by monitoring the consumption of the NADH cofactor at 340 nm (Figure S10). Apparent Michaelis—Menten constants of 0.39 ± 0.08 mM and 57.85 ± 17.8 μM for glucose and NADH substrates, respectively, evidenced enzyme-like first order kinetic behavior (Figure S11). Additionally, the NADH oxidation rate depended linearly on the concentration of NanoNOx ($^{app}k_{cat,NADH} = 498 \pm 14\ min^{-1}$, Figure S12). In comparison to other described NADH (per)oxidase-like artificial systems, ours showed the highest apparent turnover number found in literature (Table 1). Remarkably, when contrasted with the reported hemin-based Nox mimetics, i.e., hemin/G-quadruplex hybrid, NanoNOx showed up to 2000 times higher activity towards NADH oxidation. We hypothesize that such improvement might arise from the combination of several benefits exhibited by our system. First, NanoNOx permits high loads of organometallic catalyst per enzyme. Further, the accommodation of iron porphyrins through metal-ligand coordination to imidazole ligands resembles the strategy chosen by Nature to design hemoproteins and boosts the efficiency of the system.[20,27] Finally, the confinement of the catalysts in the nanospace permits the in situ injection of H_2O_2 from the core towards the iron porphyrin through a guided diffusion mechanism.

We ascertained the stability of NanoNOx in presence of organic solvents. The tolerance to high concentrations (50 %, v/v) of organic solvents such as methanol (MeOH), acetone (ACE), tetrahydrofuran (THF), and acetonitrile (MeCN) was evaluated. As displayed in Figure 1A, the catalytic activity of NanoNOx remained high, between 50 and 75 % of the performance in aqueous solution (Fig-

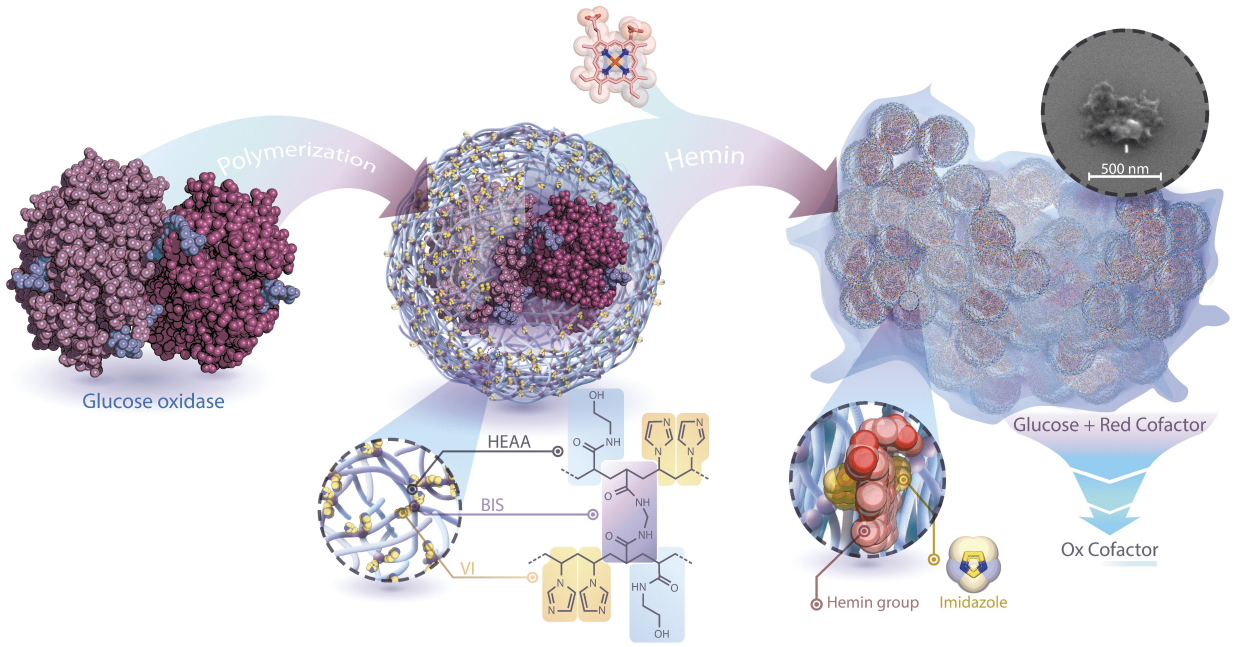

Scheme 1. Synthesis workflow of NanoNOx. In a first step, GOx is encapsulated within a thin and porous nanogel, which is synthesized in situ on the surface of the protein using N-hydroxyethylacrylamide (HEAA) and vinyl imidazole (VI) as co-monomers and N,N′-Methylenebisacrylamide (BIS) as the crosslinker. Next, the polymer is loaded with hemin catalysts through metal-ligand coordination to the imidazole moieties. The optimal addition of hemin renders solid materials by the hemin-directed crosslinking of individual nanogels (details in scanning electron microscope inset image). In the presence of glucose, a concurrent cascade reaction is implemented within the hybrid material, releasing oxidized nicotinamide cofactors to the medium.

Table 1: Reported apparent turnover numbers ($^{(app)}k_{cat}$) of assorted artificial and enzymatic systems capable of oxidizing NADH.

Mechanism	System	Composition	$^{(app)}k_{cat}$ [min^{-1}]	Refs.
Peroxidase	Artificial	Hemin/G-quadruplex	0.276	[11]
	Artificial	Ru-MOG	164	[28]
	Artificial	Cu@Cu_2O aerogel	32.6	[29]
	Enzymatic	NADH peroxidase	1400	[30]
	Enzymatic	Myoglobin/scopoletin	7.85	[10]
Oxidase	Artificial	Hemin/G-quadruplex	0.006	[11]
	Artificial	PtNP@MWCNT	1.26	[31]
	Artificial	Synthetic metalloporphyrin	6.6	[32]
	Artificial	PEI/ZIF-FMN	2.9	[33]
	Enzymatic	NADH oxidase	6198	[5]
	Semiartificial (chemoenzymatic)	Heterogeneous NanoNOx	498	This study

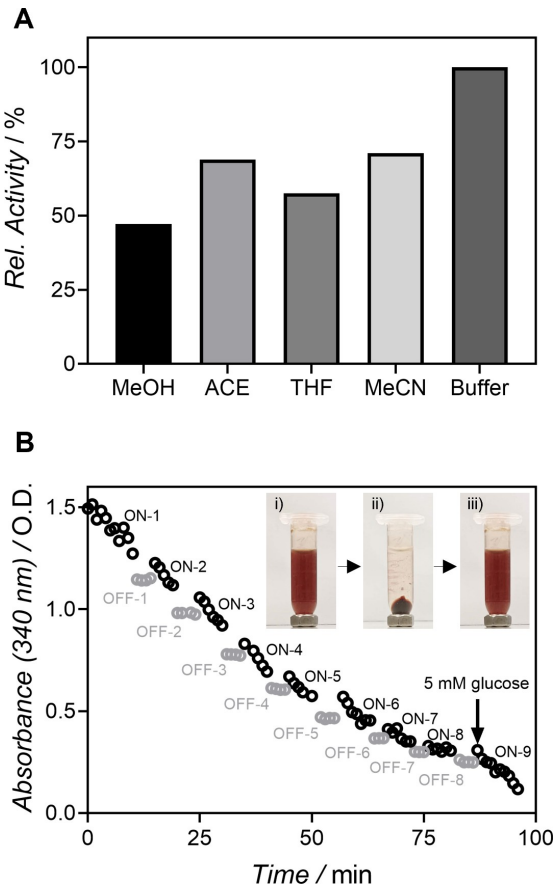

Figure 1. Catalytic performance of NanoNOx. A) NanoNOx activity in the presence of 50% (v/v) organic solvents (methanol (MeOH), acetone (ACE), tetrahydrofurane (THF), and acetonitrile (MeCN)). B) ON-OFF switching experiment to evaluate the reusability of NanoNOx. The inset images show a dispersion of NanoNOx (i), the solid material after centrifugation (ii), and NanoNOx after redispersion (iii).

ure S13). These results suggest that NanoNOx are a valuable alternative to labile Nox for the NAD-dependent biosynthesis of insoluble molecules.[3]

Next, the reusability of heterogeneous NanoNOx was tested following the ON/OFF switching activity assay (Figure 1B). The ON phase started by the addition of NanoNOx to a glucose/NADH solution. After 5 minutes, NanoNOx was removed by centrifugation (10000 rcf, 3 min). The steady concentration of NADH in the medium (OFF phase) evidenced that the oxidation of NADH was completely stopped, which proves a successful removal of the catalyst from the medium. Note that there is a recurrent absorbance-drop between the ON and OFF phases of around 0.1. This is due to the NanoNOx intrinsic absorbance at 340 nm (Figure S8), which is completely removed by centrifugation in each of the OFF cycles. The ON/OFF switching procedure was repeated nine times and a continuous kinetic trend could be observed. Importantly, after reaching the equilibrium, a steady-state kinetic is recovered upon the addition of extra substrate, i.e., 5 mM of glucose, (3.25 vs 2.94 $\mu M min^{-1}$, for ON-1 and ON-9 cycles, respectively, Table S2).

All the catalytic results discussed above are based on the extinction of NADH. Nevertheless, non-selective oxidations or overoxidation of the cofactors would likewise be monitored as a drop in the measurements at 340 nm.[34] Importantly, such non-selective oxidation of NADH would imply the unsuitability of NanoNOx as recycling system. Conversely, the oxidation selectivity of NanoNOx assessed by ^{1}H-NMR spectroscopy (Figure 2) unequivocally evidences the yield of the biologically relevant oxidized cofactor, i.e., the 1,4-NAD^+ regioisomer (Figure 2I and ii). Moreover, the oxidized cofactor was isolated and subsequently utilized by a NAD-dependent alcohol DH from *Bacillus stearothermophilus* (BsADH; PDB: 1RJW) with success (Figure S14).

Only few wild nOx are capable of oxidizing both phosphorylated and/or synthetic cofactors, so there is considerable interest in developing universal nicotinamide regeneration artificial systems.[35] In this work, we have explored the ability of NanoNOx to oxidize both NADPH and a synthetic cofactor, i.e.,1-benzyl-1,4-dihydronicotinamide (BNAH), which is bioactive, cheaper and more stable than natural cofactors.[36,37] The oxidation of NADPH by NanoNOX displayed a meaningful catalytic performance ($^{app}k_{cat} = 273 \pm 5\ min^{-1}$, Figure S15), similar to that found in evolved mutant NADPH oxidases.[38] Moreover, the oxidation of BNAH was certainly efficient. NanoNOx showed 37 to 103 times higher activity than artificial systems, i.e.,

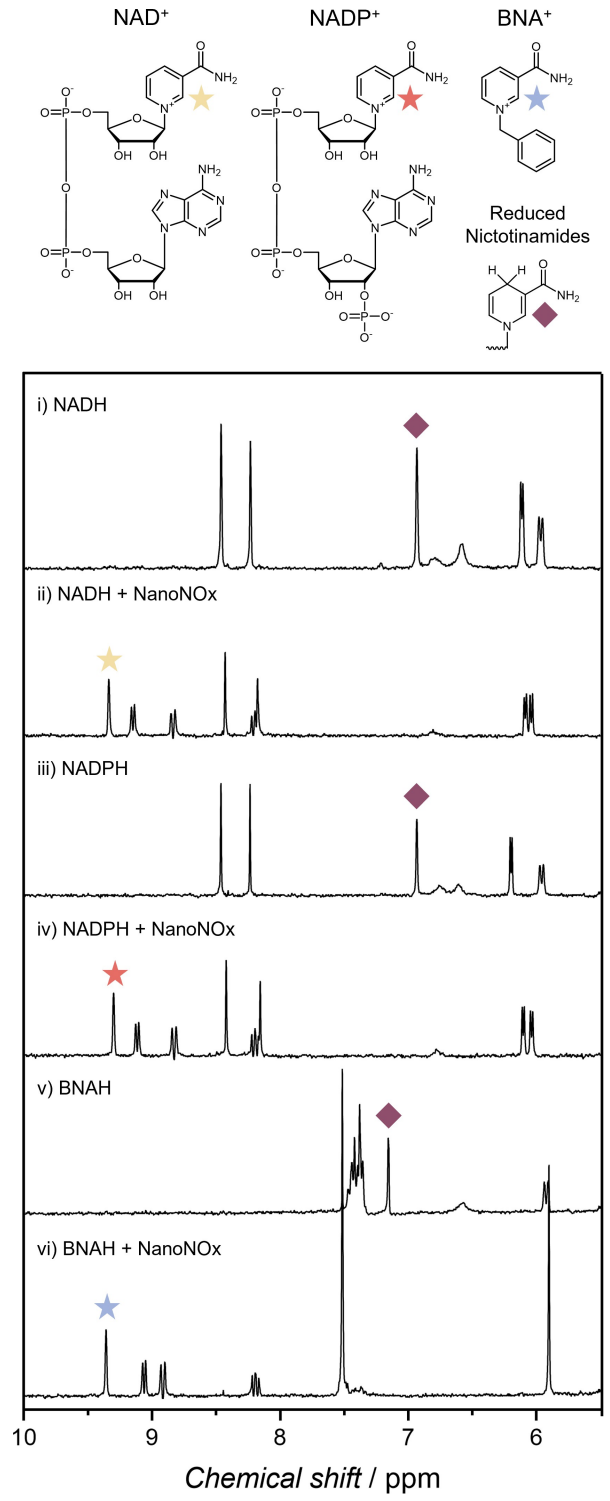

Figure 2. Chemical structures of nicotinamide cofactors and changes in their ^{1}H-NMR spectra after oxidation with NanoNOx. i) NADH; ii) oxidized NADH (NAD^+); iii) NADPH; iv) oxidized NADPH ($NADP^+$); v) BNAH; and vi) oxidized BNAH (BNA^+). Stars designate monitored hydrogens of the biologically active nicotinamide moiety. Purple rhombuses indicate the singlet attributed to the H-2 of the nicotinamide ring of the reduced cofactors.

PtNP@MWCNT, hemoproteins, and reported nOx with BNAH oxidation ability ($^{app}k_{cat} = 374 \pm 20\ min^{-1}$, Figure S16 and Figure S17).[10,31,39] Importantly, a regio-selective oxidation of NADPH and BNAH was achieved, giving rise to the formation of biologically active cofactors (Figure 2ii—vi). Overall, these results highlight the extraordinary performance and the unparalleled versatility of NanoNOx to oxidize nicotinamide-based cofactors.

Further, we assessed the feasibility of heterogeneous NanoNOx as NADH regeneration system in combination with BsADH enzyme for the oxidation of benzyl alcohol (BnOH) to benzaldehyde. In a successful recycling, our nOx biomimetic would keep the cofactor pool in its oxidized form, namely, NAD^+ (Figure 3A). In a first one-pot experiment, we aimed at converting 10 mM of BnOH by adding 1 mM of NAD^+ and 20 mM of glucose to the reaction mixture without (orange rhombus) and with (red circles) NanoNOx (Figure 3B). After 2 h of reaction, the non-recycled system reached low yields, with only 2.3 % of the BnOH oxidized (Figure S18). The addition of NanoNOx to the reaction (optimized amount of 0.25 U ml^{-1}, Figure S19) prompted the yield to 19 %, which gives a total turnover number (TTN) of almost 2 for NAD^+ (Figure 3B, red circles). However, the reaction progress was stopped after 2 h. A ^{1}H-NMR inspection of the reaction mixture evidenced that the NADH cofactor is fully oxidized at this stage, ready to be utilized by the BsADH enzyme (Figure S20). With this information, we hypothesized that the progression of the reaction could be affected by the inactivation of the biocatalyst due to the accumulation of hydrogen peroxide in the reaction medium. Thus, the BsADH was isolated from the reaction and characterized. We determined a drop in the initial catalytic performance of ca. 38 % using isopropanol as substrate (Figure S21). Further, in a separate experiment, we observed that 5 mM of H_2O_2 decreased the activity of BsADH around 35 % (Figure S22), which also supported our hypothesis. We observed that the accumulation of hydrogen peroxide also damaged the NanoNOx (29.4 %, Figure S23).

A high concentration of hydrogen peroxide in the medium reflects an unbalanced catalytic equilibrium among all the catalytic figures. Here, the oxidation performed by NanoNOx is faster than the oxidation of BnOH accomplished by BsADH, which leads to the accumulation of hydrogen peroxide in the reaction milieu (Figure 3C, left). Therefore, in a next experiment sequence, we sought to reach a balanced catalytic equilibrium by lowering the transformation rate of NanoNOx by means of a step-wise addition of glucose to the reaction. We envisioned that this approach would reduce the release of hydrogen peroxide to the medium, thereby minimizing the inactivation of the (bio)catalysts (Figure 3C, right). The supply of glucose (fuel injections of 0.2 mM) every 5 min raised the oxidation performance to 67 % (final concentration of glucose of 20 mM, Figure 3B, black squares). When the doses were spaced every 15 min, the reaction rate decreased, but satisfyingly, a conversion of ca. 95 % was obtained in 24 h (Figure 3B, green triangles). We attribute the improvement of the conversion to the controlled diffusion of hydrogen

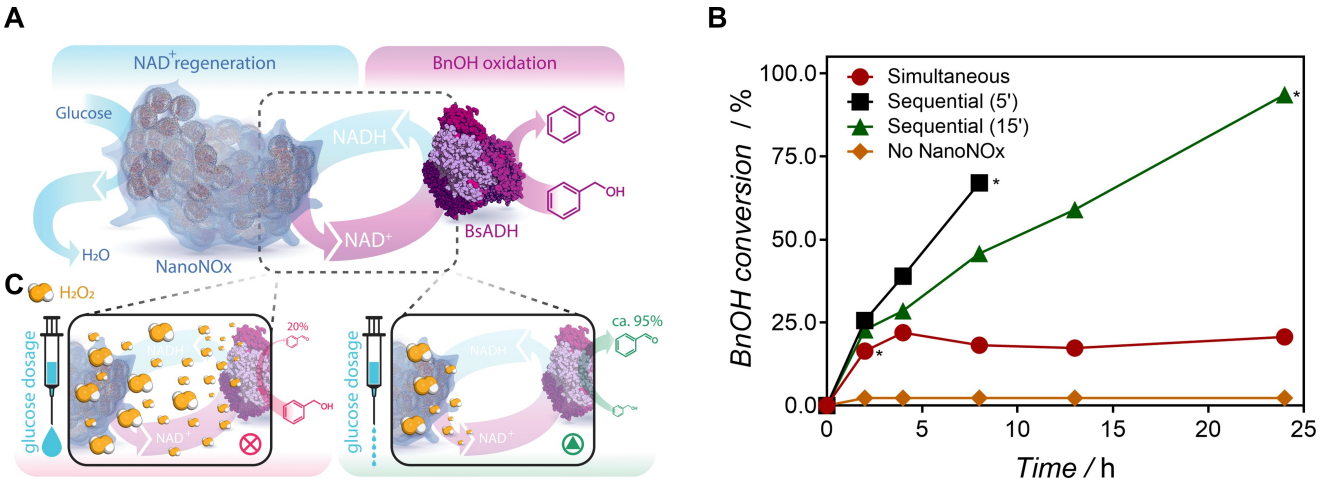

Figure 3. Study of the applicability of NanoNOx in NAD-dependent coupled oxidations. A) Illustration of coupled NanoNOx-BsADH biocatalytic system for the formation of NADH and the concomitant regeneration of NAD^+ that boosts the oxidation of BnOH. B) BnOH oxidation kinetics with different glucose addition modes: simultaneous (20 mM), 0.2 mM every 5 min, 0.2 mM every 15 min, and without NanoNOx. Asterisks represent the point at which [glucose] = 20 mM. C) A single dose of glucose generates copious amounts of H_2O_2 in the medium, which halts the reaction progress (left). The sequential addition of small concentrations of glucose generates low levels of H_2O_2, which are directionally channelled to the organometallic catalysts without damaging the biomolecules present in the reaction (right).

peroxide within NanoNOx. Under low fuel concentrations, the hydrogen peroxide is predominantly used by the hemin molecules to oxidize NADH rather than being released to the medium of reaction (Figure S24).[40] Finally, we aimed to upscale the reaction to 50 mM of BnOH. The sequential addition of glucose gave rise to a conversion of BnOH of ca. 50 % and a TTN of 25 for NAD^+ after 24 h (Figure S25). Remarkably, these yields are comparable to reported values for the enzymatic oxidation of BnOH by NOx-BsADH pairs.[41,42] Interestingly, we demonstrated the versatility of NanoNOx in combination with L-lactic dehydrogenase (LDH) enzyme for the synthesis of pyruvate using L-lactate as substrate. In this case, the NanoNOx-LDH system converted ca. 20 % of 50 mM of lactate (TTN of 10) after 8 h of reaction (Figure S26).

In summary, we have designed and fabricated a versatile semiartificial chemoenzymatic heterogeneous catalyst able to efficiently mimic NOx enzymes. To the best of our knowledge, NanoNOx show the highest turnover number of all the artificial systems reported. Albeit NanoNOx display lower catalytic activity than NOx in terms of $k_{cat,NADH}$, its high solvent tolerance, robustness, easy recyclability, and its performance in the oxidation of both NADPH and BNAH makes this chemoenzymatic system an attractive approach for the in situ recycling of cofactors. A profound optimization of NanoNOx as a cofactor recycling system unveiled that the confined architecture permits the in situ injection of H_2O_2 towards the iron porphyrin catalyst. A controlled experimental design based on the step-wise supply of glucose allows for the reduction of harmful peroxide released to the environment. Overall, the nanomaterial developed in this work opens new avenues for the implementation of hybrid chemoenzymatic catalysts in the recycling of oxidized nicotinamide cofactors, which will be of immense help in NAD(P)-dependent biotransformations.

Acknowledgements

The authors thank Prof. Fernando López-Gallego for providing the BsADH enzyme and Dr. Desiré Di Silvio for XPS measurements. The authors gratefully acknowledge the financial support from the Spanish Research Agency (AEI) for the financial support (PID2019-110239RB-I00 from I+D call and RYC2018-025923-I from RyC program), including FEDER funds; IKERBASQUE-Basque Foundation for Science, BBVA foundation (Leonardo Fellowships, IN[21]_CBB_QUI_0086) and Maria de Maeztu Units of Excellence Programme: Grant Number CEX2020-001038-M. AR-A thanks the Basque Government for his Ph.D. fellowship (PRE_2021_2_0151). Open Access funding is provided by the University of the Basque Country (UPV/EHU).

Conflict of Interest

The authors declare no conflict of interest.

Data Availability Statement

The data that support the findings of this study are available in the supplementary material of this article.

Keywords: Cascade Reactions · Chemoenzymatic Materials · Heterogeneous Biocatalysis · Nicotinamide Cofactor Regeneration

[1] S. Wu, R. Snajdrova, J. C. Moore, K. Baldenius, U. T. Bornscheuer, *Angew. Chem. Int. Ed.* **2021**, *60*, 88–119; *Angew. Chem.* **2021**, *133*, 89–123.

[2] H. Wu, C. Tian, X. Song, C. Liu, D. Yang, Z. Jiang, *Green Chem.* **2013**, *15*, 1773–1789.

[3] C. Rodriguez, I. Lavandera, V. Gotor, *Curr. Org. Chem.* **2012**, *16*, 2525–2541.

[4] G. Rehn, A. T. Pedersen, J. M. Woodley, *J. Mol. Catal. B* **2016**, *134*, 331–339.

[5] J. D. Zhang, Z. M. Cui, X. J. Fan, H. L. Wu, H. H. Chang, *Bioprocess Biosyst. Eng.* **2016**, *39*, 603–611.

[6] H. Maid, P. Böhm, S. M. Huber, W. Bauer, W. Hummel, N. Jux, H. Gröger, *Angew. Chem. Int. Ed.* **2011**, *50*, 2397–2400; *Angew. Chem.* **2011**, *123*, 2445–2448.

[7] K. Lim, Y. S. Lee, O. Simoska, F. Dong, M. Sima, R. J. Stewart, S. D. Minteer, *ACS Appl. Mater. Interfaces* **2021**, *13*, 10942–10951.

[8] B. C. Ma, L. Caire da Silva, S. M. Jo, F. R. Wurm, M. B. Bannwarth, K. A. I. Zhang, K. Sundmacher, K. Landfester, *ChemBioChem* **2019**, *20*, 2593–2596.

[9] H. X. Liao, H. Y. Jia, J. R. Dai, M. H. Zong, N. Li, *ChemSusChem* **2021**, *14*, 1687–1691.

[10] H. Y. Jia, M. H. Zong, G. W. Zheng, N. Li, *ACS Catal.* **2019**, *9*, 2196–2202.

[11] E. Golub, R. Freeman, I. Willner, *Angew. Chem. Int. Ed.* **2011**, *50*, 11710–11714; *Angew. Chem.* **2011**, *123*, 11914–11918.

[12] Y. Li, Z. G. Wang, H. Li, B. Ding, *ChemistrySelect* **2018**, *3*, 10900–10904.

[13] R. Qu, L. Shen, A. Qu, R. Wang, Y. An, L. Shi, *ACS Appl. Mater. Interfaces* **2015**, *7*, 16694–16705.

[14] C. B. Gale, M. A. Brook, *Adv. Funct. Mater.* **2021**, *31*, 2105453.

[15] J. N. Rodriguez-Lopez, J. Hernández-Ruiz, F. Garcia-Cánovas, R. N. F. Thorneley, M. Acosta, M. B. Arnao, *J. Biol. Chem.* **1997**, *272*, 5469–5476.

[16] S. Zhou, L. Jiang, J. Zhang, P. Zhao, M. Yang, D. Huo, X. Luo, C. Shen, C. Hou, *Microchim. Acta* **2021**, *188*, 160.

[17] E. T. Hwang, S. Lee, *ACS Catal.* **2019**, *9*, 4402–4425.

[18] Y.-Q. Zhang, T.-T. Feng, Y.-F. Cao, X.-Y. Zhang, T. Wang, M. R. Huanca Nina, L.-C. Wang, H.-L. Yu, J.-H. Xu, J. Ge, Y.-P. Bai, *ACS Catal.* **2021**, *11*, 10487–10493.

[19] F. Rudroff, M. D. Mihovilovic, H. Gröger, R. Snajdrova, H. Iding, U. T. Bornscheuer, *Nat. Catal.* **2018**, *1*, 12–22.

[20] M. Vázquez-González, C. Wang, I. Willner, *Nat. Catal.* **2020**, *3*, 256–273.

[21] D. P. Debecker, V. Smeets, M. Van der Verren, H. Meersseman Arango, M. Kinnaer, F. Devred, *Curr. Opin. Green Sustainable Chem.* **2021**, *28*, 100437.

[22] X. Li, X. Cao, J. Xiong, J. Ge, *Small* **2020**, *16*, 1902751.

[23] T. Uno, A. Takeda, S. Shimabayashi, *Inorg. Chem.* **1995**, *34*, 1599–1607.

[24] A. Rodriguez-Abetxuko, M. C. Morant-Minana, M. Knez, A. Beloqui, *ACS Omega* **2019**, *4*, 5172–5179.

[25] A. Rodriguez-Abetxuko, D. Sánchez-deAlcázar, A. L. Cortajarena, A. Beloqui, A. Rodriguez-Abetxuko, D. Sánchez-deAlcázar, A. L. Cortajarena, A. Beloqui, *Adv. Mater. Interfaces* **2019**, *6*, 1900598.

[26] A. Rodriguez-Abetxuko, P. Muñumer, M. Okuda, J. Calvo, M. Knez, A. Beloqui, *Adv. Funct. Mater.* **2020**, *30*, 2002990.

[27] Y. W. Lin, J. Wang, *J. Inorg. Biochem.* **2013**, *129*, 162–171.

[28] L. He, Y. Li, Q. Wu, D. M. Wang, C. M. Li, C. Z. Huang, Y. F. Li, *ACS Appl. Mater. Interfaces* **2019**, *11*, 29158–29166.

[29] P. Ling, Q. Zhang, T. Cao, F. Gao, *Angew. Chem. Int. Ed.* **2018**, *57*, 6819–6824; *Angew. Chem.* **2018**, *130*, 6935–6940.

[30] E. J. Crane, D. Parsonage, A. Claiborne, *Biochemistry* **1996**, *35*, 2380–2387.

[31] H. Song, C. Ma, L. Wang, Z. Zhu, *Nanoscale* **2020**, *12*, 19284–19292.

[32] H. Maid, P. Böhm, S. M. Huber, W. Bauer, W. Hummel, N. Jux, H. Gröger, *Angew. Chem. Int. Ed.* **2011**, *50*, 2397–2400; *Angew. Chem.* **2011**, *123*, 2445–2448.

[33] J. Chen, Q. Ma, M. Li, W. Wu, L. Huang, L. Liu, Y. Fang, S. Dong, *Nanoscale* **2020**, *12*, 23578–23585.

[34] A. W. Harris, O. Yehezkeli, G. R. Hafenstine, A. P. Goodwin, J. N. Cha, *ACS Sustainable Chem. Eng.* **2017**, *5*, 8199–8204.

[35] B. Petschacher, N. Staunig, M. Müller, M. Schürmann, D. Mink, S. De Wildeman, K. Gruber, A. Glieder, *Comput. Struct. Biotechnol. J.* **2014**, *9*, e201402005.

[36] C. E. Paul, S. Gargiulo, D. J. Opperman, I. Lavandera, V. Gotor-Fernández, V. Gotor, A. Taglieber, I. W. C. E. Arends, F. Hollmann, *Org. Lett.* **2013**, *15*, 180–183.

[37] C. E. Paul, D. Tischler, A. Riedel, T. Heine, N. Itoh, F. Hollmann, *ACS Catal.* **2015**, *5*, 2961–2965.

[38] P. B. Brondani, H. M. Dudek, C. Martinoli, A. Mattevi, M. W. Fraaije, *J. Am. Chem. Soc.* **2014**, *136*, 16966–16969.

[39] C. Nowak, B. Beer, A. Pick, T. Roth, P. Lommes, V. Sieber, *Front. Microbiol.* **2015**, *6*, 957.

[40] C. Chen, M. Vázquez-González, M. P. O'Hagan, Y. Ouyang, Z. Wang, I. Willner, *Small* **2022**, *18*, 2104420.

[41] S. Velasco-Lozano, J. Santiago-Arcos, J. A. Mayoral, F. López-Gallego, *ChemCatChem* **2020**, *12*, 3030–3041.

[42] J. Santiago-Arcos, S. Velasco-Lozano, E. Diamanti, A. L. Cortajarena, F. López-Gallego, *Front. Catal.* **2021**, *1*, 715075.

Manuscript received: May 11, 2022
Accepted manuscript online: June 28, 2022
Version of record online: July 13, 2022